# Modeling the magnetosphere for northward interplanetary magnetic field: effects of electrical resistivity

Joachim Raeder

Institute of Geophysics and Planetary Physics, University of California, Los Angeles

**Abstract.** We develop a simple analytic model and use global simulations of Earth's magnetosphere to investigate the effects of electrical resistivity on the topology of the magnetosphere for northward interplanetary magnetic field (IMF). We find that for low resistivity values ($\lesssim 10^4\,\Omega$ m) the magnetosphere remains open after 6 hours of northward IMF. For larger values ($\gtrsim 2\times10^5\,\Omega$ m) the magnetic flux of the tail lobes decreases rapidly on the timescale of $\sim$1 hour. In this case the tail becomes closed, tadpole-shaped, steady state, and of finite length. The tail length decreases with increasing resistivity and becomes as short as about 50 $R_E$ for a resistivity value of $10^6\,\Omega$ m. Reconnection between IMF and lobe field lines occurs in all cases and is not significantly affected by the resistivity. However, large values of the resistivity annihilate lobe flux and break the frozen-in condition for closed tail flux tubes, leading to a decoupling of the flux tube motion from plasma convection. These effects make the development of a steady, closed tail of finite length possible. Because resistivity values larger than $10^2\,\Omega$ m are unrealistic for the quiet time tail, we conclude that the magnetosphere is unlikely to ever close and that models which predict the rapid closure and a steady, finite length tail are possibly in error due to numerical resistivity.

## 1. Introduction

The structure and magnetic topology of the magnetosphere under northward IMF conditions is one of the fundamental problems in magnetospheric physics. Under such conditions, magnetospheric activity ceases and the magnetosphere attains a ground state that sets the stage for new episodes of activity. While it is now well accepted that the magnetosphere has an open magnetic topology during periods of southward IMF [*Cowley*, 1980] (i.e., many magnetospheric field lines are connected with the interplanetary magentic field (IMF)), a completely different (namely, a closed) topology appears to be possible under northward IMF conditions [*Cowley*, 1983; *Troshichev*, 1990].

During periods of southward IMF, magnetic reconnection between IMF and magnetospheric field lines is the predominant solar wind-magnetosphere coupling mechanism [*Cowley*, 1980]. There is now increasing evidence that reconnection is also an important coupling process during northward IMF conditions [*Kessel et al.*, 1996; *Berchem et al.*, 1995]. For the latter case, magnetic reconnection takes place be-tween IMF and lobe field lines at high latitude. In fact, such a reconnection process has been predicted previously by several phenomenological models [*Cowley*, 1983; *Crooker*, 1992; *Dungey*, 1963; *Troshichev*, 1990; *Song and Russell*, 1992; *Russell*, 1972; *Reiff*, 1982; *Reiff and Burch*, 1985; *Kan and Burke*, 1985; *Kivelson*, 1982]. However, these models differ greatly with respect to the resulting magnetic topology of the magnetosphere and treat for the most part only steady state situations. *Cowley* [1983] and *Troshichev* [1990] summarize the various possible magnetic topologies that may result from lobe reconnection. Some of these models predict a closed magnetosphere as a result of the merging process; however, closed models all require that reconnection occurs simultaneously and symmetrically both at the northern and southern lobes. It has been argued that such a situation is very unlikely [*Russell*, 1972], and consequently, the magnetosphere will never close.

However, some indirect experimental evidence appears to be consistent with a closed magnetosphere during intervals of prolonged northward IMF. Using ISEE 3 data from the

distant tail, *Fairfield* [1993] finds that ISEE 3 encounters the tail lobes less often than expected for northward IMF. He notes that this would be consistent with a closed magnetosphere and a tail length of $\lesssim 200\ R_E$ during these intervals. In a separate study using Geotail data, *Fairfield et al.* [1996] found that during an extended period of time ($\sim 10$ hours), Geotail did not observe plasma and fields typical of the tail although the spacecraft was well positioned in the distant tail around $X_{\mathrm{GSE}} = $ -134 $R_E$. He argues that these observations are consistent with a closed magnetosphere at that time. Other evidence may be found in polar cap precipitation data. Solar electrons (polar rain), which are thought to be an indicator of open field lines (field lines that connect with the solar wind at one end) [*Fairfield and Scudder*, 1985], are sometimes found absent in the polar cap region [*Riehl and Hardy*, 1986; *Newell et al.*, 1997]. However, other studies have reported the presence of polar rain even in periods of magnetospheric quiescence and strong northward IMF [*Frank et al.*, 1986; *Gussenhoven and Mullen*, 1989; *Makita et al.*, 1985; *Hoffman et al.*, 1988]. Thus the question of a closed magnetosphere can at present not be answered experimentally, given the limitations of the available data sets. In fact, it even remains questionable whether any experiment can address the question successfully because a null result (the disappearance of the tail lobes or the polar cap) is required, which is notoriously difficult to obtain as it would require measurements of very high spatial density.

In spite of the uncertainties about magnetospheric topology during northward IMF, several studies using global simulations of the magnetosphere have been performed [*Usadi et al.*, 1993; *Watanabe and Sato*, 1990; *Tanaka*, 1995; *Ogino et al.*, 1992, 1994; *Fedder and Lyon*, 1995; *Raeder et al.*, 1995; *Gombosi et al.*, 1998]. The majority of these studies finds that the magnetosphere closes after $\sim 1$ hour of northward IMF. One should keep in mind, however, that all of these studies use highly idealized simulation setups, i.e., the solar wind and IMF parameters are kept steady and no dipole tilt is considered. The only study so far that did predict an open magnetosphere after several hours of constant northward IMF was presented by *Raeder et al.* [1995]. That study found, similar to other simulation studies, that magnetic reconnection occurs at the lobes in both hemispheres in a symmetric fashion. However, the reconnection rate was very low, leading to the persistence of open lobe flux even after 4 hours of due northward IMF. The other studies, although not all of them present a detailed analysis, predict such symmetric lobe reconnection as well but also lead to a very rapid closure of the magnetosphere after the IMF turns northward. Although none of the simulation studies estimates the reconnection rate explicitly, one is led to speculate that the models which close rapidly simply exhibit higher re-

connection rates. This, of course, is likely to be true as the models employ different parameters and also differ greatly by the numerical schemes that they use to solve the MHD equations. As we shall show in the next sections, however, magnetic diffusion may play the dominant role in some of the models and may be the cause the rapid closing of the magnetosphere after northward IMF turnings. In this paper we therefore examine the issue of magnetic diffusion in global models of Earth's magnetosphere in detail. In section 2 we discuss the effects of reconnection and magnetic diffusion on the magnetosphere. In section 3 we briefly describe our model, and in section 4 we present results that show how different amounts of magnetic diffusion affect the magnetospheric topology. Finally, in section 5 we summarize and discuss our results.

## 2. Magnetic Diffusion Versus Reconnection

For the magnetosphere to close, open magnetic flux of the tail lobes has to be converted into closed flux, i.e., the magnetic topology of the tail has to change. For obvious reasons, this change cannot be a continuous deformation of the magnetic field but must involve the cutting and reattachment of field lines. Thus the frozen-in condition $\mathbf{E} = -\mathbf{v} \times \mathbf{B}$ must be violated, and other terms in Ohm's law must play an important role. For reconnection to take place it is generally assumed that the dominant nonideal term in Ohm's law is the resistivity, although other terms, like a nonvanishing divergence of the electron pressure tensor, may also be invoked [*Hesse et al.*, 1995; *Kuznetsova et al.*, 1995]. Whatever mechanism breaks the frozen-in condition, it only needs to be operative in a very limited spatial region. In the classical picture of fast reconnection [*Petschek*, 1964] this region is located around the magnetic X line and called the diffusion region. At the X line field lines are then cut and reattached, although most of the energy conversion is thought to take place in the slow mode shocks that fan out from the diffusion region itself. Thus the essence of reconnection is that the violation of the frozen flux condition need only to occur in a very limited spatial region.

Let us now assume that magnetic diffusion is not restricted to a small spatial region but is operative everywhere, or almost everywhere, in the magnetosphere. The assumption of ideal MHD needs then to be replaced with resistive MHD, and the time evolution of the magnetic field is then governed (assuming spatially homogeneous resistivity $\eta$) by

$$\frac{\partial \mathbf{B}}{\partial t} = \nabla \times \{-\mathbf{v} \times \mathbf{B} + \eta \mathbf{j}\} \qquad (1)$$

$$\frac{\partial \mathbf{B}}{\partial t} = -\nabla \times (\mathbf{v} \times \mathbf{B}) + \frac{\eta}{\mu_0} \nabla^2 \mathbf{B} \qquad (2)$$

or, in the absence of convection, by

$$\frac{\partial \mathbf{B}}{\partial t} = \frac{\eta}{\mu_0}\nabla^2 \mathbf{B} \qquad (3)$$

Because we are mostly concerned with the diffusion of the tail lobe field, we may further simplify (3) by assuming that the only spatial dependence is in the $z$ direction and that the dominant field component is in the $x$ direction; thus

$$\frac{\partial B_x}{\partial t} = \frac{\eta}{\mu_0}\frac{\partial^2 B_x}{\partial z^2} \qquad (4)$$

With the initial condition $B_x(z \leq 0,0) = B_{x1}$ and $B_x(z > 0,0) = B_{x2}$, the initial value problem has the solution

$$B_x(z,t) = B_{x1} +$$
$$\frac{1}{2}(B_{x2} - B_{x1})\left\{1 - \text{erf}\left(\frac{z}{2\sqrt{\eta t/\mu_0}}\right)\right\} \qquad (5)$$

where $\text{erf}(x)$ is the error function [*Abramowitz and Stegun*, 1970], defined as

$$\text{erf}(x) = \frac{2}{\sqrt{\pi}}\int_0^x e^{-t^2}dt \qquad (6)$$

Figure 1 shows solutions of equation (5) after 0.25, 0.5, 1, 2, 4, and 8 hours for resistivities ranging from $10^2$ to $10^6\ \Omega$ m. For $\eta = 10^2\ \Omega$ m and $\eta = 10^3\ \Omega$ m the initial current sheet broadens only slightly, to no more than about 3 $R_E$ after 8 hours. A resistivity of $10^4\ \Omega$ m causes considerably more broadening, leading to roughly the same width after one hour as the $10^3\ \Omega$ m case leads to after 8 hours. Resistivities of $10^5\ \Omega$ m and $10^6\ \Omega$ m lead to a rapid broadening of the current sheet even after only 1 hour or less. Apparently, there is a transition at about $10^4$-$10^5\ \Omega$ m between resistivities that would have only a minor effect on the tail topology ($\lesssim 10^4\ \Omega$ m) and such that should have a profound effect on the tail ($\gtrsim 10^5\ \Omega$ m). In order to assess the effect of large resistivities on the tail topology in more detail we perform global simulations of the magnetosphere which entail the effects explicitly in the induction equation.

## 3. Model

We use a global MHD code which includes an ionospheric model for the closure of field-aligned currents [*Raeder et al.*, 1997, 1998]. In order to accommodate the large simulation volume with a long tail and long simulation times the simulation code was parallelized for running on multiple instruction-multiple data (MIMD) machines by using a domain decomposition technique [*Fox et al.*, 1988]. The model

solves the ideal MHD equations (modified as described below) for the magnetosphere and a potential equation for the ionosphere. Numerical effects, such as diffusion, viscosity, and resistivity, are necessarily introduced by the numerical methods. These permit viscous interactions and to a limited extent magnetic field reconnection. For this study we keep an explicit resistivity term in Ohm's law, which is discussed in more detail below.

### 3.1. Outer Magnetosphere

The magnetospheric (MHD) part of the model is solved using a finite difference method which is conservative for the gasdynamic part of the MHD equations:

$$\frac{\partial \rho}{\partial t} = -\nabla \cdot (\rho \mathbf{v}) \qquad (7)$$

$$\frac{\partial \rho \mathbf{v}}{\partial t} = -\nabla \cdot (\rho \mathbf{vv} + p\mathsf{I}) + \mathbf{j} \times \mathbf{B} \qquad (8)$$

$$\frac{\partial e}{\partial t} = -\nabla \cdot (\{e + p\}\mathbf{v}) + \mathbf{j} \cdot \mathbf{E} \qquad (9)$$

$$\frac{\partial \mathbf{B}}{\partial t} = -\nabla \times \mathbf{E} \qquad (10)$$

$$\nabla \cdot \mathbf{B} = 0 \qquad (11)$$

$$\mathbf{E} = -\mathbf{v} \times \mathbf{B} + \eta \mathbf{j} \qquad (12)$$

$$\mathbf{j} = \nabla \times \mathbf{B} \qquad (13)$$

$$e = \frac{1}{2}\rho v^2 + \frac{p}{\gamma - 1} \qquad (14)$$

where $\rho$ is the plasma density, $\mathbf{v}$ is the velocity, $p$ is the plasma pressure, $\mathsf{I}$ is the unit tensor of rank 3, $e$ is the plasma energy density, $\gamma$ is the specific heat ratio (a value of 5/3 is used in these simulations), $\mathbf{B}$ is the magnetic field, $\mathbf{j}$ is the current density, $\mathbf{E}$ is the electric field, and $\eta$ is the electrical resistivity. Note that all variables are normalized to reference values in order to eliminate numerical factors such as the permeability of free space.

The $\mathbf{j} \times \mathbf{B}$ and $\mathbf{E} \cdot \mathbf{j}$ terms are treated as source terms because the very low plasma $\beta$ and the large magnetic field gradients near Earth do not allow the use of the full conservative form of the MHD equations. The electrical resistivity $\eta$ is either held constant or given by a model of anomalous resistivity:

$$\eta = \alpha j'^2 \quad \text{if} \quad j' \geq \delta, \quad \eta = 0 \quad \text{otherwise} \qquad (15)$$

$$j' = \frac{|j|\Delta}{|B| + \epsilon} \qquad (16)$$

where $j$ is the local current density, $B$ is the local magnetic field, $\Delta$ is the grid spacing, and $\epsilon$ is a very small number ($10^{-8}$) introduced to avoid dividing by zero. The normalized current density $j'$ ($0 \leq j' \leq 1$) is used as a switch
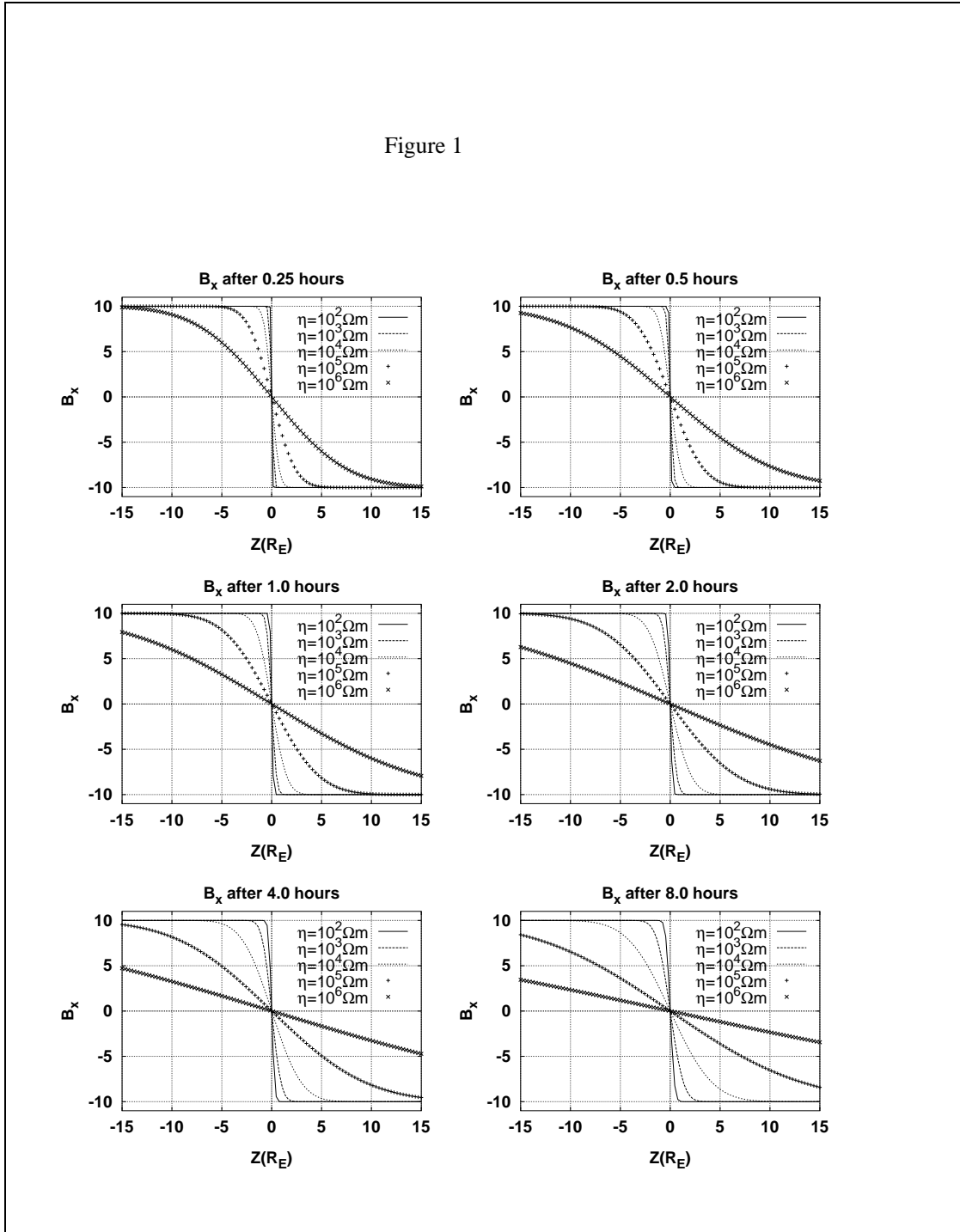
**Figure 1.** Solutions of equation (5) for different resistivity values and at six different times (0.25, 0.5, 1, 2, 4, and 8 hours).

for the resistivity. In places where the resistivity is switched on, it becomes proportional to the square of the local current density. Similar resistivity models have been used in the past to model the kinetic effects that lead to anomalous resistivity [*Sato and Hayashi*, 1979; *Hoshino*, 1991]. The parameters $\alpha$ and $\delta$ determine the value of the resistivity and the current density threshold that must be reached for the resistivity to be switched on. The parameter $\delta$ ($\delta$=0.75 in these simulations) is chosen such that the resistivity $\eta$ is nonzero only at a very few grid points in strong current sheets. The dimensionless parameter $\alpha$ has a value of 0.05 for the simulations shown in this paper. With this choice of $\alpha$ the largest possible value for $\eta$ is $\eta_{max}$=$3 \times 10^6 \Omega$ m. Because $\eta$ depends on the local plasma parameters, its value varies strongly both in time and space. Typically, at any given time, only a few tens to a few hundreds grid cells (out of about $10^6$) reach values larger than one tenth of $\eta_{max}$.

The numerical grid is rectangular and nonuniform with the highest spatial resolution (about 0.5 $R_E$) near Earth. It extends 20 $R_E$ in the sunward direction, 400 $R_E$ in the tailward direction, and $\pm 50$ $R_E$ in the $Y$ and $Z$ directions. The gasdynamic part of the equations is spatially differenced by using a technique in which fourth-order fluxes are hybridized with first-order (Rusanov) fluxes [*Harten and Zwas*, 1972; *Hirsch*, 1990]. The magnetic induction equation is treated somewhat differently [*Evans and Hawley*, 1988] in order to conserve $\nabla \cdot \mathbf{B} = 0$ exactly. The time stepping scheme for all variables consists of a low-order predictor with a time-centered corrector, which is accurate to the second order in time. The outer boundary conditions are fixed at the given solar wind values on the upstream side. At the other boundaries we apply open, i.e., zero normal derivative, boundary conditions.

### 3.2. Ionosphere

The inner boundary, where the MHD quantities are connected to the ionosphere, is taken to be a shell of radius 3.7 $R_E$ centered at Earth. The choice of this radius is a compromise necessitated by numerical considerations, such as very high Alfvén speeds and very large magnetic field gradients closer to Earth. However, this choice allows for the proper mapping of all relevant field-aligned current (FAC) systems down to $\sim 59°$ magnetic latitude. The placement of the inner boundary also inhibits the formation of a ring current. Inside this shell we do not solve the MHD equations but assume a static dipole field. The important physical processes earthward of that shell are the flow of FACs and the closure of these currents in the ionosphere. Every few time steps (corresponding to a time interval of $< 5$ s in real time) we use the static dipole field to map the magnetospheric FACs from the 3.7 $R_E$ shell onto the polar cap. We then use the

FACs as input for the ionospheric potential equation:

$$\nabla \cdot \Sigma \cdot \nabla \Phi = -j_{\parallel} \sin I \qquad (17)$$

which is solved on the surface of a sphere with a radius of 1.015 $R_E$. Here $\Phi$ denotes the ionospheric potential as a function of magnetic latitude and local time, $\Sigma$ is the tensor of the ionospheric conductance, $j_{\parallel}$ is the mapped FAC with the downward current considered positive and corrected for flux tube convergence, and $I$ is the inclination of the dipole field at the ionosphere. The boundary condition $\Phi = 0$ is applied at the equator. Although more sophisticated models are available for the ionospheric Pedersen and Hall conductance [*Raeder et al.*, 1998], we use here a uniform Pedersen conductance of 5 S and zero Hall conductance. The uniform conductance ensures that the ionospheric convection pattern remains symmetric about the noon-midnight meridian, whereas a model with gradients in the conductance would break the symmetry, even if the IMF is due northward. For the same reason we choose not to include any dipole tilt, i.e., the dipole axis in the model coincides with the GSE $z$ axis. Using the mapped FACs and ionospheric conductances, the potential equation is solved using a pseudo spectral Galerkin method [*Canuto et al.*, 1987], and the ionospheric potential is mapped to the 3.7 $R_E$ shell where it is used as a boundary condition for the magnetospheric flow by taking $\mathbf{v} = (-\nabla \Phi) \times \mathbf{B} / B^2$.

### 3.3. Initial Conditions

The initial conditions for the magnetic field are constructed from the superposition of Earth's dipole over an equally strong mirror dipole, such that $B_x$ vanishes at $x = 16$ $R_E$. Sunward of the plane of symmetry at 16 $R_E$ the field is replaced by the initial solar wind field. This procedure ensures a divergence-free transition from the constant solar wind field to the magnetospheric field. The simulation box is initially filled with tenuous (0.1 cm$^{-3}$) and cold (5000 K) plasma of zero velocity. The simulation run is started with a southward IMF in order to let the unphysical initial conditions evolve into a magnetospheric configuration. After 2 hours we flip the IMF into a due northward direction without changing any of the other parameters. We then continue to run the model for 6 more hours under due northward IMF conditions.

## 4. Simulation Results

We have run the model for several different resistivity parameters which are listed in Table 1.

The solar wind parameters are identical for all runs ($V_{SW}$

**Table 1.** Simulation Runs

| Run | Resistivity, $\Omega$ m | $R_M$[b] |
|-----|------------------------|----------|
| A | NL[a] | $\infty$ |
| B | $10^3$ | 2400 |
| C | $10^4$ | 240 |
| D | $10^5$ | 24 |
| E | $2\times10^5$ | 12 |
| F | $3\times10^5$ | 8 |
| G | $6\times10^5$ | 4 |
| H | $10^6$ | 2.4 |

[a] Nonlinear model (see equations (9) and (10)).

[b] Magnetic Reynolds number $R_M = L_0 V_0/\eta$ based on $L_0 = 1\ R_E$ and $V_0 = 300$ km/s.

= 420 km/s, $N_{SW} = 6.5\ cm^{-3}$, $P_{SW} = 1.8 \times 10^{-12}$ Pa, $B_{x,SW}, B_{y,SW} = 0$, $B_{z,SW} = \pm$ 5nT).

Plates 1a-1h show renderings of the magnetospheric configuration 8 hours into the simulation runs, i.e., after 6 hours of due northward IMF. The equatorial plane shows the color-coded plasma pressure, with red depicting the highest values; yellow, green, and blue depicting intermediate values; and magenta depicting the lowest values. The plane at $x = -100\ R_E$ shows the magnetic topology. Orange areas are threaded by unconnected field lines, blue areas are threaded by open (i.e., lobe) field lines, and pink areas are threaded by closed field lines. The light pink surface encloses volumes of closed flux, i.e., it depicts the open-closed boundary. The ripples on those surfaces are a numerical artifact due to the finite resolution grid (The surfaces are produced by assigning a value of 1 to every grid point that lies on a closed field line and else a value of -1. The surface shown is then the isosurface for the value 0.)

Plate 1a shows the magnetic topology for the case in which the resistivity is given by the nonlinear model (equations (15) and (16)). This run (run A) essentially reproduces the result of *Raeder et al.* [1995]. Most of the tail consists of closed field lines, except for a region around the midnight meridian where open flux is still present. This open flux fills a slot in the closed flux volume that extends from the cusp near the terminator into the distant tail. Reconnection between IMF and lobe field lines is occurring just tailward of the cusps and produces new closed field lines at the expense of the remaining lobe flux. However, this process must be fairly slow, otherwise, the lobe flux should already have disappeared. Because of the symmetries there is no process operating in this case that could produce new lobe flux. This

may not generally be true in reality, however, where dipole tilt, a finite IMF $B_x$ component, or a finite IMF $B_y$ component is present. In those cases, the symmetry of reconnection between the northern and southern hemispheres may be broken and reconnection may then produce new open flux from previously closed flux tubes [see, e.g., *Cowley*, 1983, Figure 8d].

Plates 1b (run B) and 1c (run C) show the magnetospheric topology for the cases of $10^3\ \Omega$ m and $10^4\ \Omega$ m uniform resistivity in Ohm's law (equation (11)), respectively. For these two cases the magnetic topology is virtually the same as in run A. Considering that the nonlinear resistivity model produces a finite resistivity only in very few places where the local current exceeds the threshold (typically at a few grid points around a X line), cases A-C appear to be dominated by numerical resistivity to the effect that the added resistivity terms produce no noticeable change.

The case of $10^5\ \Omega$ m uniform resistivity (run D, Plate 1d) is distinctly different from the previously discussed cases. There are still tail lobes left; however, they are now much smaller than in the cases A, B, and C. There is also a slot in the closed field line volume that emerges from the cusps, and thus reconnection is occurring there. However, as will be seen in the cases of even higher resistivity, reconnection does not necessarily occur between IMF and open field lines but may at least in part be occurring between closed field lines and the IMF. The latter process will also produce a slot as seen in Plate 1d.

When the resitivity is increased further, the magnetic topology changes profoundly. Plates 1e-1h show the topology for runs E to H with resistivities of $2 \times 10^5\ \Omega$ m, $3 \times 10^5\ \Omega$ m, $6 \times 10^5\ \Omega$ m, and $10^6\ \Omega$ m, respectively. For all
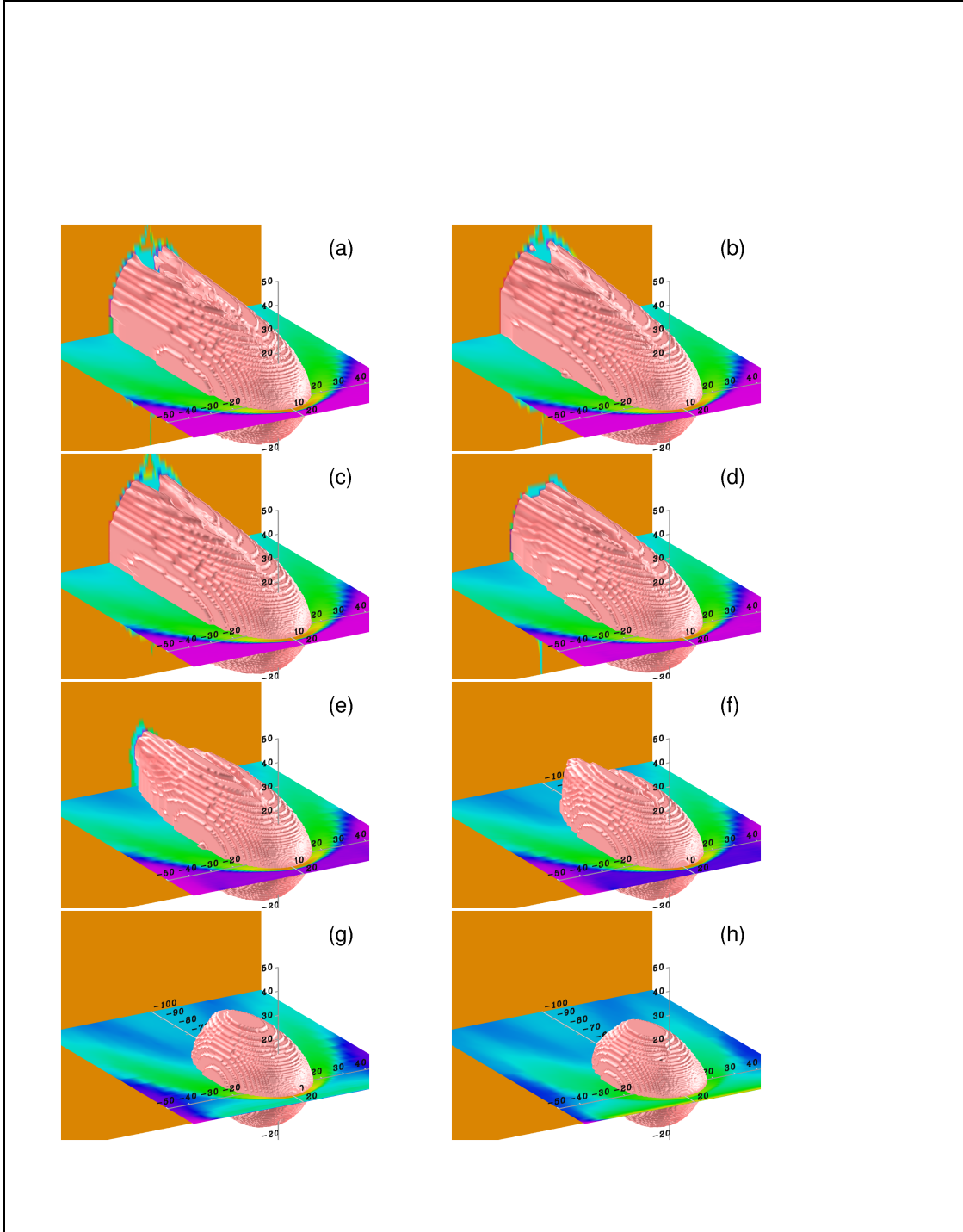
**Plate 1.** Rendering of the magnetosphere showing the plasma pressure in the equatorial plane, the magnetic topology at $X=-100\ R_E$, and the open-closed boundary (pink surface) for (a) model run A with anomalous resistivity, (b) model run B with a constant resistivity of $10^3\ \Omega$ m, (c) $10^4\ \Omega$ m, (d) $10^5\ \Omega$ m, (e) $2\times10^5\ \Omega$ m, (f) $3\times10^5\ \Omega$ m, (g) $6\times10^5\ \Omega$ m, and (h) $10^5\ \Omega$ m. See text for details.

of these cases the magnetosphere is closed. The tail length decreases with increasing values of the resistivity. For $\eta = 2 \times 10^5 \; \Omega$ m the tail is $\sim$110 $R_E$ long, for $\eta = 3 \times 10^5 \; \Omega$ m the tail length is $\sim$80 $R_E$, and becomes as short as $\sim$50 $R_E$ for the highest value of resistivity ($10^6 \; \Omega$ m). In cases E and F the shape of the magnetosphere is approximately that of a tadpole. Also, in these cases there is still a slot visible at high latitudes in the closed flux volume. This slot is due to reconnection between closed flux tubes and the IMF. No net change of closed flux occurs by this reconnection process. A closed flux tube that is removed by this process is replaced by a new closed flux tube that extends across the dayside. The other two ends of the originally closed flux tube are then disconnected and form the slots that are visible in Plates 1e and 1f. In the cases of the higher resistivity (Plates 1g and 1h) the magnetosphere takes the shape of a bubble. There is also no high-latitude slot, indicating that reconnection is not operating at high latitudes in these cases but is completely swamped by field diffusion.

The time evolution of run A is shown in Plates 2a-2f. Plate 2a shows the topology shortly before the IMF turns northward. Because the IMF has been due southward for $\sim$2 hours, there is a tail X line located at about $x = -25$ $R_E$. As the northward IMF reaches the dayside magnetopause (Plate 2b), lobe reconnection begins and starts to form a LLBL (Low Latitude Boundary Layer) type layer around the frontside magnetopause. As time progresses, this layer expands both in width and tailward (Plates 2c and 2d). While the initial formation of this boundary layer occurs rapidly, it takes several hours for this broad layer (which has been termed previously the tail flank boundary layer (TFBL) [*Raeder et al.*, 1995]) to engulf the tail lobes and partially replace them (Plates 2e and 2f).

In case of run F the initial time development is similar to run A (Plates 3a and 3b), with the exception that the initial southward IMF X line lies closer to Earth at about $x = -18$ $R_E$. However, after 160 min, i.e., 20 min after the northward turning of the IMF (Plate 3c), the tail is noticeably different from case A at the same time (Plate 2c). There is also a TFBL which is comparable to the TFBL in case A, but the tail lobes are much smaller at this time compared to case A. The similarity of the TFBL in both runs indicates that the lobe reconnection process works quite similar in both cases. The much more rapidly shrinking lobes in case F, however, appear to be caused by magnetic diffusion. If the rapid shrinkage were caused by faster high-latitude lobe reconnection, the TFBL in case F should be much broader and reflect the larger amount of reconnected lobe flux. After 224 min the tail lobes have disappeared in case F, and the tail has become closed with a finite length of $\sim$180 $R_E$ (Plate 3d). As time progresses, the tail then becomes shorter until

it eventually reaches an approximate steady state with a tail length of $\sim$80 $R_E$ (Plates 3e and 3f).

In both cases A and F the closed flux in the TFBL is produced by symmetric reconnection of IMF field lines with lobe field lines at high latitude. However, the time evolution of that closed flux is different in these two cases. In case A the closed flux, which is initially immersed in the magnetosheath plasma, is carried into the distant tail. We attribute the different motions of the flux tubes in cases A and F to be primarily due to magnetic diffusion. In effect, the diffusion breaks the frozen-in condition of ideal MHD and lets the field lines slip through the plasma. Thus the motion of the field lines becomes partially decoupled from the motion of the plasma which makes the development of a finite size, closed magnetosphere possible.

## 5. Summary and Discussion

We have used a simple analytic model and global MHD simulations of Earth's magnetosphere to study the effect of finite resistivity on the topology of the magnetotail. The analytic model indicates that magnetic diffusion can annihilate lobe flux in a matter of a few hours if the resistivity exceeds about $10^5 \; \Omega$ m. The global simulations confirm this finding.

For southward IMF conditions the flux annihilation is balanced by new open flux that is generated due to magnetic reconnection at the dayside; thus the magnetic topology of the tail does not change qualitatively and the magnetosphere remains open.

For northward IMF, no such replenishing of lobe flux occurs. Instead, reconnection between lobe and IMF field lines converts open flux tubes of the lobes into closed flux tubes as discussed by *Cowley* [1983]. Without diffusion, this process leads to a broad boundary layer in the tail flanks (TFBL) which convects tailward. Enhanced diffusion does not alter the lobe-IMF reconnection in a significant way. However, diffusion has additional effects that profoundly alter the tail topology. First, diffusion annihilates additional lobe flux, which leads to a rapid disappearance of the tail lobes. Second, the convection of the closed flux in the TFBL becomes partially decoupled from the plasma convection because the frozen-in condition is no longer valid. This causes the tail ends of these flux tubes eventually to stop convecting tailward. Without additional resistivity the TFBL flux tubes continue to convect tailward because of the momentum flux of the magnetosheath flow in which they are embedded.

The combination of these two effects, diffusion of the tail lobe field and the violation of the frozen-in condition in the TFBL, leads to the rapid formation of a steady state magnetotail of finite length. Without the additional annihilation of lobe flux due to diffusion the tail would also close even-
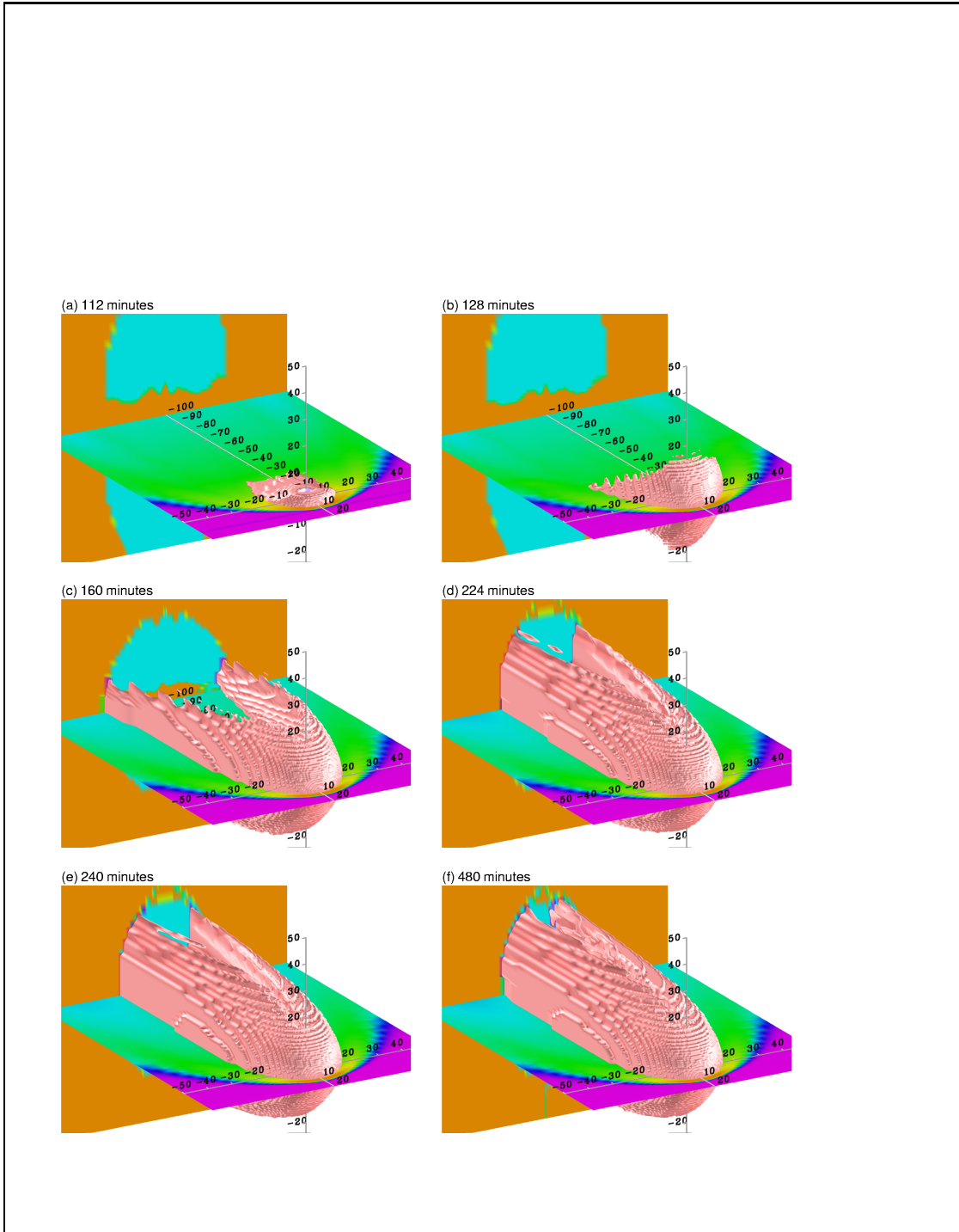
**Plate 2.** Time sequence of the magnetosphere configuration for run A with anomalous resistivity. Note that the IMF turns northward at 120 min.
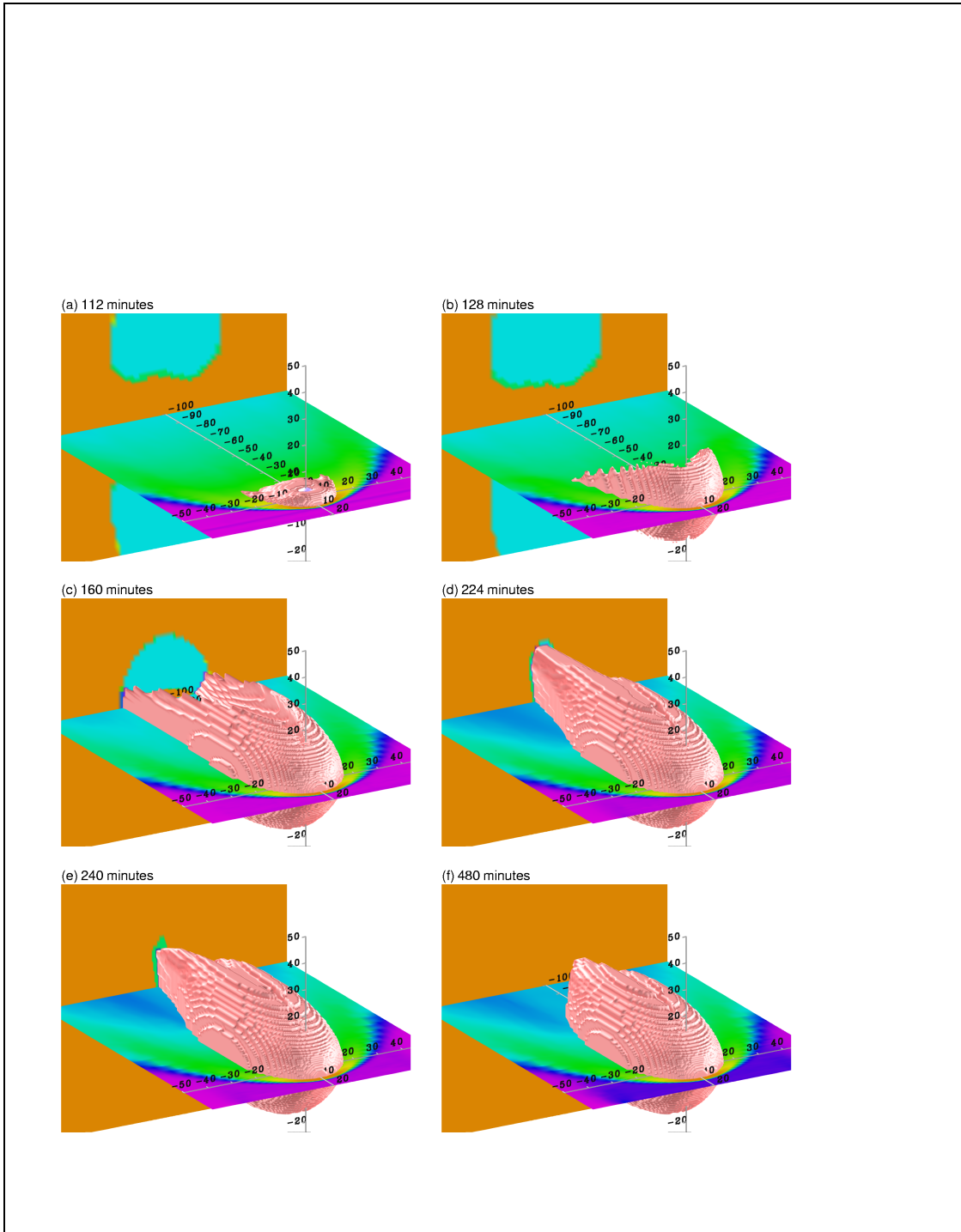
**Plate 3.** Time sequence of the magnetosphere configuration for run F with $3 \times 10^5$ $\Omega$ m uniform resistivity. Note that the IMF turns northward at 120 min.

tually by virtue of high-latitude reconnection; however, this process would take much longer. Since our baseline model (A), which still contains numerical resistivity, does not close after 6 hours of northward IMF, this process would probably require a steady northward IMF of 10 hours or more. If, on the other hand, the frozen-in condition is not violated in the TFBL, the tail might still close but would not be steady state because the tail ends of the TFBL flux tubes would continue to convect tailward.

Of course, electrical resistivity values of the order of $10^5 \, \Omega$ m or more are hardly realistic for the entire tail. At best, anomalous resistivities of such magnitude could be expected in very limited regions of the tail current sheet during active times [*Cattell and Mozer*, 1986; *Cattell*, 1996]. For quiet times, *Cattell* [1996] found values of the Lundquist number (i.e., magnetic Reynolds number) in the tail current sheet of $10^3$ or larger, corresponding to values of the resistivity that are smaller than $10^2 \, \Omega$ m.

Thus, magnetic diffusion should play no significant role in the magnetotail during northward IMF and the following conclusions can be drawn:

1. In reality, the magnetotail will hardly ever close because stable northward IMF conditions for more than 10 hours rarely occur. Even when a 10+ hour period of northward IMF occurs, there are always IMF $B_x$ and $B_y$ components of finite magnitude. These IMF components would rather keep the magnetosphere open because they may destroy the symmetries required to close the magnetosphere by simultaneous lobe reconnection. The latter effects deserve further study by using global models.

2. A uniform resistivity in excess of about $10^5 \, \Omega$ m is sufficient to produce a rapidly closing magnetotail of finite length.

3. Model results that indicate the rapid closure and the formation of a steady state, finite length, magnetotail could possibly be caused by numerical diffusion. One should note, however, that a closed magnetotail could also result from the initial conditions. If the simulation is started with a northward IMF, there is no open tail flux to begin with. However, it is useful to keep in mind that every period of northward IMF is preceeded by a period of southward IMF. The question is not if the magnetosphere is closed, but how it closes.

4. The model problem presented in this paper can be used to obtain a rough estimate of the inherent numerical magnetic diffusion level of a global model. As long as adding a uniform resistivity of value $\eta_0$ to the model does not change the results appreciably, the inherent numerical resistivity is likely to be larger than $\eta_0$. For the model used in this study we find that $\eta_0$ is of the order of $10^4 \, \Omega$ m. One should note, however, that numerical effects are usually not homo-geneous; thus $\eta_0$ should be regarded as a lower bound.

# References

Abramowitz, M., and I. A. Stegun, *Handbook of Mathematical Functions*, Dover, Mineola, N.Y., 1970.

Berchem, J., J. Raeder, and M. Ashour-Abdalla, Magnetic flux ropes at the high-latitude magnetopause, *Geophys. Res. Lett.*, *22*, 1189, 1995.

Canuto, C., M. Y. Hussaini, A. Quarteroni, and T. A. Zang, *Spectral Methods in Fluid Dynamics*, Springer-Verlag, New York, 1987.

Cattell, C. A., Experimental evaluation of the Lundquist number for the Earth's magnetopause and magnetotail, *J. Geophys. Res.*, *101*, 27309, 1996.

Cattell, C. A., and F. S. Mozer, Experimental determination of the dominant wave mode in the active near-Earth magnetotail, *Geophys. Res. Lett.*, *13*, 221, 1986.

Cowley, S. W. H., Plasma poulations in a simple open model magnetosphere, *Space Sci. Rev.*, *26*, 217, 1980.

Cowley, S. W. H., Interpretation of observed relations between solar wind characteristics and effects at ionospheric altitudes, in *High Latitude Space Plasma Physics*, edited by B. Hultquist, and T. Hagfors, p. 225, Plenum, New York, 1983.

Crooker, N. U., Reverse convection, *J. Geophys. Res.*, *97*, 19363, 1992.

Dungey, J. W., The structure of the exosphere or adventures in velocity space, in *Geophysics, The Earth's Environment*, edited by C. DeWitt, J. Hieblot, and A. Lebeau, p. 550, Gordon and Breach, Newark, N.J., 1963.

Evans, C. R., and J. F. Hawley, Simulation of magnetohydrodynamic flows: A constrained transport method, *Astrophys. J.*, *332*, 659, 1988.

Fairfield, D. H., Solar wind control of the distant magnetotail: ISEE 3, *J. Geophys. Res.*, *98*, 21265, 1993.

Fairfield, D. H., and J. D. Scudder, Polar rain: Solar coronal electrons in the Earth's magnetosphere, *J. Geophys. Res.*, *90*, 4055, 1985.

Fairfield, D. H., R. P. Lepping, L. A. Frank, K. L. Ackerson, W. R. Paterson, S. Kokubun, T. Yamamoto, K. Tsuruda, and M. Nakamura, Geotail observations of an unusual magnetotail under very northward IMF conditions, *J. Geomag. Geoelec.*, *48*, 473, 1996.

Fedder, J. A., and J. G. Lyon, The Earth's magnetosphere is 165 $R_E$ long: Self-consistent currents, convection, magnetospheric structure, and processes for northward interplanetary magnetic field, *J. Geophys. Res.*, *100*, 3623, 1995.

Fox, G. C., M. A. Johnson, G. A. Lyzenga, S. W. Otto, J. K. Salmon, and D. W. Walker, *Solving Problems on Concurrent Processors*, Prentice Hall, Englewood Cliffs, N.J., 1988.

Frank, L. A., et al., The theta aurora, *J. Geophys. Res.*, *91*, 3177, 1986.

Gombosi, T. I., D. L. DeZeeuw, C. P. T. Groth, K. G. Powell, and P. Song, The length of the magnetotail for northward IMF: Results of 3D MHD simulations, in *Phys. Space Plasmas (1998)*, edited by T. Chang, and J. R. Jasperse, vol. 15, p. 121, Cambridge, Mass., 1998.

Gussenhoven, M. S., and E. G. Mullen, Simultaneous relativistic electron and auroral particle access to the polar caps during interplanetary magnetic field $B_z$ northward: A scenario for an open field line source of auroral particles, *J. Geophys. Res.*, *94*, 17121, 1989.

Harten, A., and G. Zwas, Self-adjusting hybrid schemes for shock computations, *J. Comput. Phys.*, *9*, 568, 1972.

Hesse, M., D. Winske, and M. M. Kuznetsova, Hybrid modeling of collisionless reconnection in two-dimensional current sheets: Simulations, *J. Geophys. Res.*, *100*, 21815, 1995.

Hirsch, C., *Numerical Computation of Internal and External Flow*, vol. II, John Wiley, New York, 1990.

Hoffman, R. A., M. Suguira, N. C. Maynard, R. M. Candey, J. D. Craven, and L. A. Frank, Electrodynamic patterns in the polar region during periods of extreme magnetic quiescence, *J. Geophys. Res.*, *93*, 14515, 1988.

Hoshino, M., Forced magnetic reconnection in a plasma sheet with localized resistivity profile excited by lower hybrid drift type instability, *J. Geophys. Res.*, *96*, 11555, 1991.

Kan, J. R., and W. J. Burke, A theoretical model of polar cap auroral arcs, *J. Geophys. Res.*, *90*, 4171, 1985.

Kessel, R. L., S.-H. Chen, J. L. Green, S. F. Fung, S. A. Boardsen, L. C. Tan, T. E. Eastman, J. D. Craven, and L. A. Frank, Evidence of high-latitude reconnection during northward IMF: Hawkeye observations, *Geophys. Res. Lett.*, *23*, 583, 1996.

Kivelson, M. G., July 29, 1977, Magnetospheric studies: Impulsive waves, global dynamics and geomagnetic indices, *J. Geophys. Res.*, *87*, 5981, 1982.

Kuznetsova, M. M., M. Hesse, and D. Winske, Hybrid modeling of the tearing instability in collisionless two-dimensional current sheets: Linear theory, *J. Geophys. Res.*, *100*, 21827, 1995.

Makita, K., C. I. Meng, and S. I. Akasofu, Temporal and spatial variations of the polar cap dimension inferred from the precipitation boundaries, *J. Geophys. Res.*, *90*, 2744, 1985.

Newell, P. T., D. Xu, C.-I. Meng, and M. G. Kivelson, Dynamical polar cap: A unifying approach, *J. Geophys. Res.*, *102*, 127, 1997.

Ogino, T., R. J. Walker, and M. A. Ashour-Abdalla, A global magnetohydrodynamic simulation of the magnetosheath and magnetosphere when the interplanetary magnetic field is northward, *IEEE Trans. Plasma Sci.*, *20*, 817, 1992.

Ogino, T., R. J. Walker, and M. Ashour-Abdalla, A global magnetohydrodynamic simulation of the response of of the magnetosphere to a northward turning of the interplanetary magnetic field, *J. Geophys. Res.*, *99*, 11027, 1994.

Petschek, H. E., Magnetic field annihilation, in *The Physics of Solar Flares*, edited by W. N. Hess, p. 425, NASA Spec. Publ. SP-50, 1964.

Raeder, J., et al., Boundary layer formation in the magnetotail: Geotail observations and comparisons with a global MHD model, *Geophys. Res. Lett.*, *24*, 951, 1997.

Raeder, J., R. J. Walker, and M. Ashour-Abdalla, The structure of the distant geomagnetic tail during long periods of northward IMF, *Geophys. Res. Lett.*, *22*, 349, 1995.

Raeder, J., J. Berchem, and M. Ashour-Abdalla, The Geospace Environment Modeling grand challenge: Results from a Global Geospace Circulation Model, *J. Geophys. Res.*, *103*, 14787, 1998.

Reiff, P. H., Sunward convection on both polar caps, *J. Geophys. Res.*, *87*, 5976, 1982.

Reiff, P. H., and J. L. Burch, $B_y$ dependent dayside plasma flow and Birkeland currents in the dayside magnetosphere, 2, A global model for northward and for southward IMF, *J. Geophys. Res.*, *90*, 1595, 1985.

Riehl, K. B., and D. A. Hardy, Average characteristics of the polar rain and their relationship to the solar wind and the interplanetary magnetic field, *J. Geophys. Res.*, *91*, 1557, 1986.

Russell, C. T., The configuration of the magnetosphere, in *Critical Problems of Magnetospheric Physics*, edited by E. R. Dyer, p. 1, Nat. Acad. of Sci., Washington, D. C., 1972.

Sato, T., and T. Hayashi, Externally driven magnetic reconnection as a powerful magnetic energy converter, *Phys. Fluids*, *22*, 1189, 1979.

Song, P., and C. T. Russell, Model of the formation of the low-latitude boundary layer for strongly northward interplanetary magnetic field, *J. Geophys. Res.*, *97*, 1411, 1992.

Tanaka, T., Generation mechanisms for magnetosphere-ionosphere current systems deduced from a three-dimensional MHD simulation of the solar wind-magnetosphere-ionosphere coupling processes, *J. Geophys. Res.*, *100*, 12057, 1995.

Troshichev, O. A., Global dynamics of the magnetosphere for northward IMF conditions, *J. Atmos. Terr. Phys.*, *52*, 1135, 1990.

Usadi, A., A. Kageyama, K. Watanabe, and T. Sato, A global simulation of the magnetosphere with a long tail: Southward and northward interplantary magnetic field, *J. Geophys. Res.*, *98*, 7503, 1993.

Watanabe, K., and T. Sato, Global simulation of the solar wind-magnetosphere interaction: The importance of its numerical validity, *J. Geophys. Res.*, *95*, 75, 1990.

J. Raeder, Institute of Geophysics and Planetary Physics, University of California, Los Angeles, 405 Hilgard Avenue, Los Angeles, CA 90095-1567. (jraeder@igpp.ucla.edu)